INTERNATIONAL JOURNAL OF CLIMATOLOGY
Int. J. Climatol. (2015)
Published online in Wiley Online Library
(wileyonlinelibrary.com) DOI: 10.1002/joc.4566

RMetS
Royal Meteorological Society

Trends in potential evapotranspiration from 1960 to 2013 for a desertification-prone region of China

Nan Shan, Zhongjie Shi,* Xiaohui Yang,* Xiao Zhang, Hao Guo, Bo Zhang and Zhiyong Zhang

Institute of Desertification Studies, Chinese Academy of Forestry, Beijing, China

ABSTRACT: Evapotranspiration is a sensitive parameter for assessing climate change. It controls energy and mass exchange and is a descriptor of drought in arid- and semi-arid regions. Using the Mann–Kendall (M–K) test, Sen's slope estimator, and the stepwise regression, temporal, and spatial variations in potential evapotranspiration (ET_0) and its dominant factors were analysed. The analysis was based on data from 173 meteorological stations in a desertification-prone region of China over the period from 1960 to 2013. The annual ET_0 decreased prior to 1990s and increased thereafter. The majority of stations had a decreasing ET_0 trend, especially in summer, in which the average slope of all stations was $-2.43\,\text{mm decade}^{-1}$. Analysis of determining factors showed that a decrease in wind speed was the primary factor associated with decreasing ET_0. The trend magnitude of ET_0 increased from $-2.25\,\text{mm decade}^{-1}$ to $-7.43\,\text{mm decade}^{-1}$ as wind speed increased, then decreased to $-3.00\,\text{mm decade}^{-1}$. Decreasing ET_0 and increasing P in the western region led to decrease in the aridity index, suggesting a wetter climate and reduced desertification. Increasing aridity index in the eastern region reduced the vegetation cover and facilitated desertification processes, which might be a disadvantage for ecological reconstruction and desertification control. Better understanding of the response of ET_0 to regional climate change may facilitate efficient use of limited water resources and establish management strategies that can combat desertification and maintain ecological security in a desertification-prone region.

KEY WORDS potential evapotranspiration; trend; attribution; Mann–Kendall test; desertification-prone region

Received 7 July 2015; Revised 19 October 2015; Accepted 20 October 2015

1. Introduction

Climate change has intensely influenced eco-hydrological cycles causing a series of water resource issues in the last few decades. Assessing the climate-induced hydrological consequence is necessary for improving water resource management and increasing the efficiency of water use. Evapotranspiration (ET), a key process controlling energy and mass fluxes exchange (Kousari and Ahani, 2012; Croitoru *et al.*, 2013), is considered to be one of the best indicators for revealing the effects of climate change on hydrological processes (Xu *et al.*, 2006; Sharifi and Dinpashoh, 2014). It also monitors the water and energy balances (Croitoru *et al.*, 2013). ET, an indispensable component of the hydrological cycle, plays a crucial role in determining the severity of drought in arid and semi-arid regions.

Desertification can easily occur in arid and semi-arid regions. It is a common problem worldwide and has drawn increasing attentions (Reynolds *et al.*, 2007; Li *et al.*, 2015). China has an extensive desertification-prone region (DPR), which is the main source area of sandstorm. Portions of this region have either been damaged by, or at risk of, desertification (Chinese Committee for Implementing UN Convention to Combat Desertification (CCICCD), 1997; Middleton and Thomas, 1997; Wang *et al.*, 2005). Due to droughts attributable to limited precipitation and improper management, the DPR is experiencing serious ecological problems and has become extremely fragile. Any minor variation in meteorological factors induced by climate change can increase the dry conditions by increasing potential evapotranspiration (ET_0) (Gan, 2000; Ma *et al.*, 2004). This may aggravate desertification and trigger sandstorms, threatening ecosystem sustainability (Huo *et al.*, 2013; Xing *et al.*, 2014). ET_0 provides useful approach to evaluate the drought intensity in some geographical regions, especially where water is the limiting factor affecting plant landscape and soil productivity (Kosmas *et al.*, 2003; Croitoru *et al.*, 2013). Under global warming conditions, identifying the spatial and temporal patterns of ET_0 variations is useful for understanding the hydrological mechanisms underlying climate change responses (Xing *et al.*, 2014). This information can contribute to better management of limited water resources and establish irrigation schemes for DPR (Wang *et al.*, 2012; Croitoru *et al.*, 2013). Assessment of climate change impact on variability of ET_0 may be helpful in determining appropriate strategies for mitigating probable damage (Shadmani *et al.*, 2012).

A warmer climate is likely to increase ET_0. However, ET_0 has recently decreased in many regions of the world

* Correspondence to: Z. Shi or X. Yang, Institute of Desertification Studies, Chinese Academy of Forestry, No. 10, Huaishuju Road, Haidian District, Beijing, China. E-mail: shijie1204@163.com; or yangxhcaf@126.com

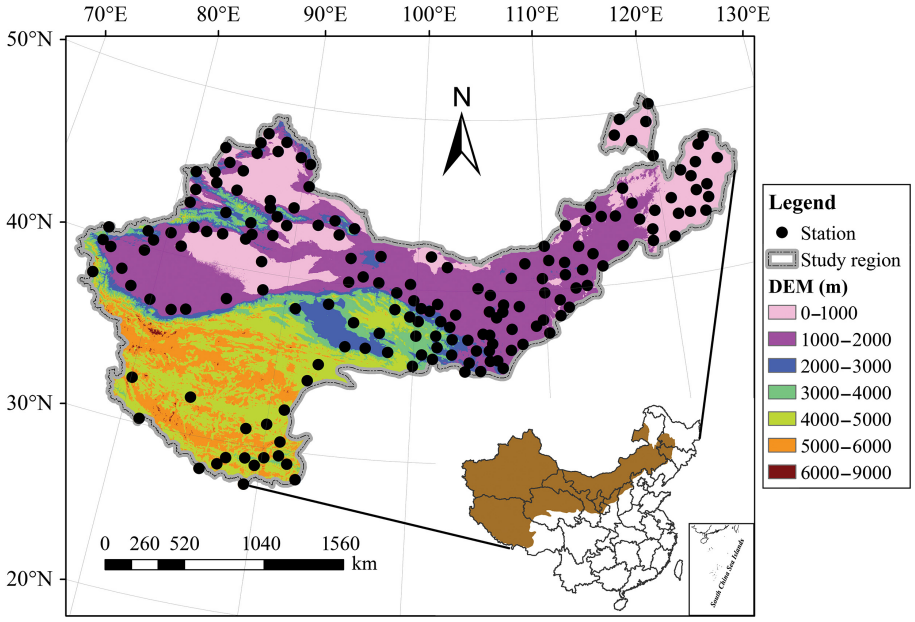

Figure 1. Location of the study area and meteorological stations.

(Roderick and Farquhar, 2005; Rayner, 2007; Irmak *et al.*, 2012; Tabari *et al.*, 2012). A disparity between expected and observed ET_0, known as the 'evapouration paradox', has been observed in semi-arid and arid regions of China (Huo *et al.*, 2013; Feng *et al.*, 2014; Li *et al.*, 2014a, 2014b). An increasing trend in ET_0 has been reported in many studies (Espadafor *et al.*, 2011; Kousari and Ahani, 2012; Berti *et al.*, 2014; Nam *et al.*, 2015). General explaining for ET_0 trends has remained elusive.

The ET_0 trend and its possible determining factors have been stimulated. In general, solar radiation and wind speed are the major determining factors. Decreases in duration of sunshine and near-land surface wind speed are termed 'global dimming and wind stilling' (Stanhill and Cohen, 2001; McVicar *et al.*, 2008). They are the dominant factors influencing the decline in ET_0 in China (Yin *et al.*, 2010) and other countries (Jhajharia *et al.*, 2012; Limjirakan and Limsakul, 2012; Tabari *et al.*, 2012). Relative humidity is the major factor causing the decline of ET_0 in some areas (Chattopadhyay and Hulme, 1997; Jung *et al.*, 2010). Climate change is spatially and seasonally heterogeneous, so regional scale trends in ET_0 and dominant factor require further study.

Although trends of ET_0 and associated meteorological variables have been studied in many regions, there is no definitive consensus on how climate change influences ET_0. In China's DPR, unique geography and extreme climate may significantly affect ET_0 trends. Accurate estimation of ET_0 and its causes are imperative for better management of limited water resources and necessary for the development of irrigation schedules for agriculture, desertification control, and environmental assessment in arid and semi-arid regions (Wang *et al.*, 2014). The objectives of this study were to (1) analyse the spatial distribution of annual and seasonal ET_0 using meteorological data from 173 stations, (2) identify trends in ET_0 and meteorological factors and determine spatial distribution and temporal change, (3) quantify the contributions of key meteorological variables to ET_0 trends, (4) identify trends in the aridity index over the DPR region of China. All these should provide favourable information that may facilitate understanding of the intensity and variations in ET_0 and meteorological factors in the DPR.

2. Materials and methods

2.1. Study area

The study area is located in northern and western China, ranging from 73.5° to 126.8°E and from 28.1° to 50.8°N. The area mainly includes Xinjiang, Ningxia, most part of Inner Mongolia, Qinghai, Gansu, Tibet, and smaller portions of western Shanxi and Shanxi, northwestern Liaoning, and Jinlin, as well as southwestern Heilongjiang. It covers an area of 4.5×10^6 km^2 (Wu *et al.*, 2007), which is about 47.1% of China. Sub-humid, semi-arid, arid, and extremely arid areas accounted for 12.6, 28.8, 34.4, and 24.2% of the region, respectively (Figure 1). Most of this region has a typical continental climate characterized by an arid climate and desertification. In the southwestern part, the Tibetan plateau has a typical plateau continental monsoon climate. The annual mean temperature is about 7.0–9.0 °C. Annual precipitation ranges from 16 and 267 mm, 80% of which occurs between June and September. Strong sunshine and high winds provide abundant solar and wind energy. The area has a complex and varied topography. This includes plateaus, plains, mountains, basins, and nearly all of China's deserts and sandy terrain, including Taklamakan Desert, Kumtag Desert, Badan Jaran Desert and so forth. It is the main source of sandstorms in China. The study area is divided into internal flow area and drain area; many lakes are mainly fed by

runoff from mountain ranges. The main vegetation cover is sandy grassland and desert, covering more than 40% of the total area. There is also farmland along rivers, interspersed with sandy grassland and oases. Moreover, there are many large-scale ecological engineering programs focused on combating the desertification and controlling dust storms in the DPR. These include the Three-North Forest Shelterbelt Program, Converting Farmland into Forest and Grassland Project, and others.

2.2. Meteorological data

Daily meteorological data collected from 1960 to 2013 at 173 weather stations were obtained from the National Climatic Centre of China Meteorological Administration (CMA) (http://www.nmic.gov.cn). Six daily meteorological variables were recorded: (1) maximum air temperature (MAT, °C), (2) minimum air temperature (MIT, °C), (3) mean relative humidity (RH, %), (4) wind speed (WS, $m\,s^{-1}$), (5) hours of sunshine (SH, h), and (6) precipitation (P, mm). The geographical location of the stations is shown in Figure 1. The data set has been checked for quality by National Meteorological Information Center (NMIC). Missing data were mainly located in Tibet and accounted for only 0.45%. These were estimated using a multiple regression relationship from neighbouring and highly correlated stations. The season was divided into spring (March to May), summer (June to August), autumn (September to November), winter (December to February), and the growing season (April to September).

2.3. Food and Agriculture Organization Penman–Monteith method

The daily ET_0 was calculated using the standard Penman–Monteith equation as recommended by the United Nations Food and Agriculture Organization (FAO) (Allen *et al.*, 1998). It has been applied successfully in many arid and semi-arid regions (Shadmani *et al.*, 2012; Liuzzo *et al.*, 2014). The equation is as follows:

$$ET_0 = \frac{0.408\Delta\left(R_n - G\right) + \gamma\left[900/\left(T+273\right)\right]U_2\left(e_a - e_s\right)}{\Delta + \gamma\left(1 + 0.34U_2\right)}$$

Here, ET_0 is the potential evapotranspiration ($mm\,day^{-1}$); R_n is the net radiation at the surface ($MJ\,m^{-2}\,day^{-1}$); G is the soil heat flux ($MJ\,m^{-2}\,day^{-1}$); T is the mean daily air temperature (°C); U_2 is the daily average wind speed at 2 m height ($m\,s^{-1}$); e_s and e_a are the saturation and actual vapour pressures (kPa), respectively; Δ is the slope of the saturated vapour pressure ($kPa°C^{-1}$); and γ is the psychrometric constant ($kPa\ °C^{-1}$). The amount of radiation was calculated using the FAO56 recommendation, in which the Angstrom coefficients of $a = 0.25$, $b = 0.5$. G is usually smaller than R_n, and it was assumed to be zero over the daily period (Allen *et al.*, 1998). Wind speed was recalculated to 2 m height based on the logarithmic wind speed profile equation (Allen *et al.*, 1998).

2.4. Trend analysis

The Mann–Kendall test (M–K test) is a rank-based non-parametric test for trend detection (Mann, 1945; Kendall, 1975). Theil–Sen's method is used to estimate the true slope and magnitude of the linear trend (Theil, 1950; Sen, 1968). The two methods offer many advantages because missing values are allowed and the data are not required to conform to any particular distribution. Single data errors and outliers do not significantly affect Sen's method (Salmi *et al.*, 2002). For this reason, they have been widely used to analyse different climatic and hydrological data series (Jhajharia *et al.*, 2012; Kousari and Ahani, 2012).

The non-parametric tests require time series to be serially independent. However, the observed meteorological data may not be independent. They displayed statistically significant serial correlations, which increased the probability of significant trends (Von Storch, 1995). The correlation component should be removed from the time series. The trend-free pre-whitening method was used to remove the correlation component from time series and eliminate the effect of serial correlation on the M–K test and Theil–Sen's slope estimator (Yue and Wang, 2004).

2.5. Identification of dominant factors

To evaluate the contributions of the meteorological variables to the ET_0, stepwise multiple regression was performed in this study (Chattopadhyay and Hulme, 1997; Han *et al.*, 2012). ET_0 was the dependent variable, MAT, MIT, RH, WS, SH, and P were the predictors. After standardization, a predictor was added to the model at the 0.05 significance level and could be regarded as the dominant factor affecting ET_0 variation.

3. Results

3.1. Spatial distribution of ET_0

Figure 2 shows the spatial distributions of annual and seasonal ET_0 from 1960 to 2013 in the DPR. The distribution of annual ET_0 showed regional differences, with higher values in the mid-northern and northwestern parts of the study area, and lower values in the mid-southern and northeastern parts of the study area. The mean annual ET_0 was 1083.9 mm and it ranged from 689.3 mm at Erguna to 1899.72 mm at Shisanjianfang. Most of the annual ET_0 values were distributed between 1000.0 mm and 1300.0 mm, with the number of stations in this range accounting for 57.80%. Only three stations of the annual ET_0 values were greater than 1600 mm. In seasonal timescale, the spatial distribution of ET_0 during the growing season was generally consistent with that of the annual ET_0, accounting for 77% of the annual total. The spatial distributions of ET_0 in spring and summer were similar to annual distribution, varying from 206.03 to 548.87 mm and from 252.64 to 908.78 mm, respectively. In winter, the stations with higher values were primarily in southwestern and northeastern parts of the study area. The

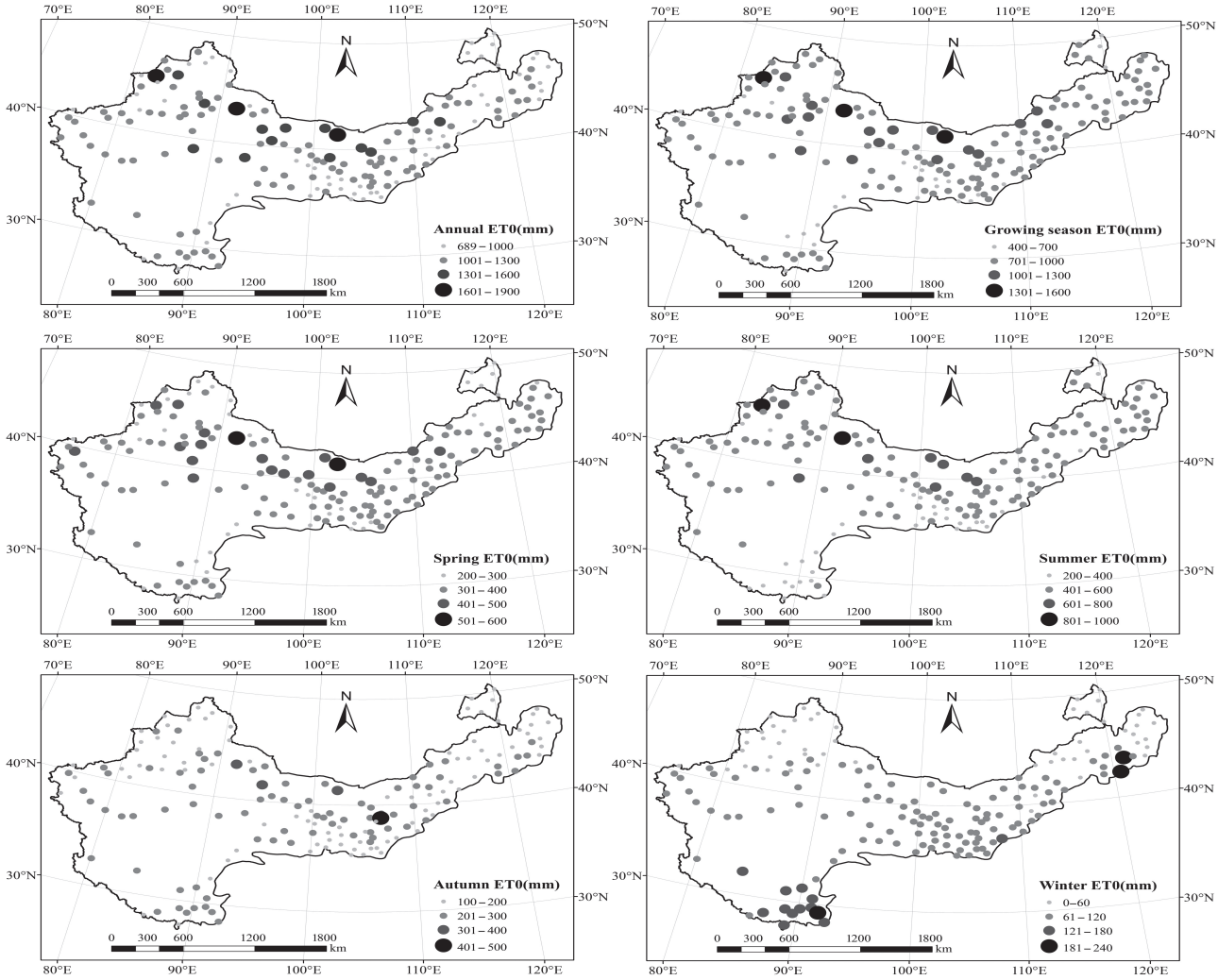

Figure 2. Spatial distributions of annual and seasonal ET_0 in the study area.

ET_0 peak among the stations was at Kailu, with a value of 229.53 mm.

3.2. Temporal variations of ET_0 and meteorological factors

The annual ET_0 showed a strong decreasing trend in the DPR from 1960 to 2013 (Figure 3). An increasing trend was observed from the 1960s to early 1970s, after which the average ET_0 decreased until 1992. This pattern was similar to that of WS and SH, especially WS, which was closely correlated with ET_0 until the 1990s ($R = 0.80$), but ET_0 showed an increase in the 1990s, followed by a decrease in the late 2000s, which corresponded to significant variations of MAT and MIT. Before the 1990s, MAT, MIT, and ET_0 showed opposite trends. Trends in RH and P were not consistent with trends in ET_0 trend from 1960 to 2013.

3.3. Spatial trends of ET_0 and meteorological factors

3.3.1. Spatial distribution of ET_0 trend

After eliminating the serial correlation effect, the annual and seasonal ET_0 trends were tested using M–K (Figure 4). The annual ET_0 showed a mix of decreasing and increasing trends. However, the decreasing trends were observed in 68.21% of the stations, which were larger than the increasing trends. The magnitudes of decreasing and increasing trends in annual ET_0 varied from -34.70 to -0.17 mm decade^{-1} and from 0.22 to 13.68 mm decade^{-1}, respectively, with an average decrease of -3.52 mm decade^{-1} across all stations. Here, 24.86% of all stations, mainly located in the eastern and northwest parts of the study area, showed significant decreasing trends at 95% confidence level and only 2.89% of all stations showed significant increasing trends at the same confidence level. Trends in the ET_0 of the growing season were similar to the annual trends for most of stations, varying from -29.94 mm decade^{-1} at Alashankou to 11.28 mm decade^{-1} at Mazongshan. There were more stations with significant increasing and decreasing trends for the growing season than with significant annual trends, 30.06 and 4.05%, respectively. Seasonal ET_0 trend analysis showed that the number of stations with significant levels varied by season. The strongest decreasing trends occurred during summer, mainly in the central and northwestern parts of the study

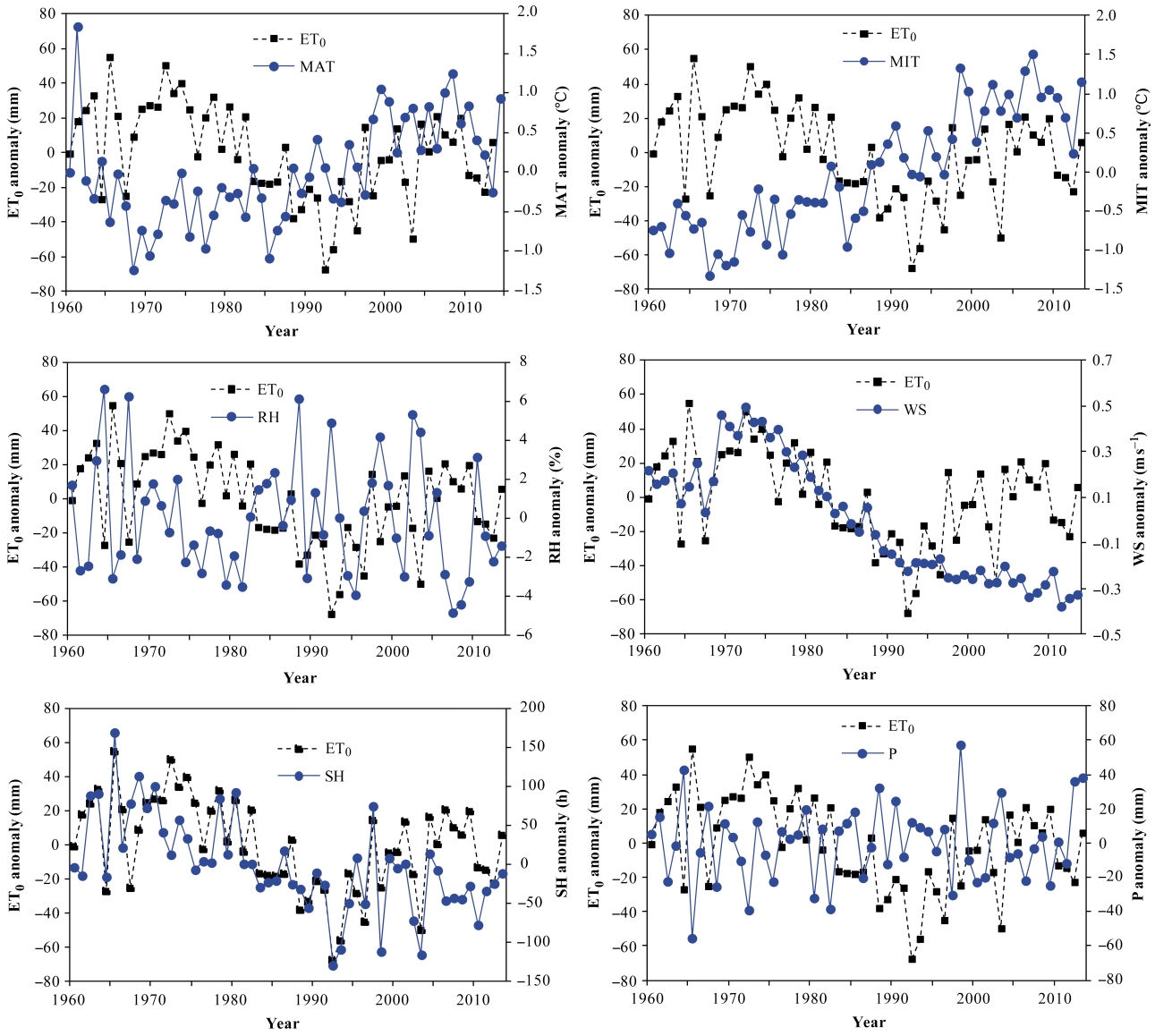

Figure 3. Annual variations of ET_0 and meteorological factors in study area from 1960 to 2013.

area, accounting for 68.78% of all stations. A total of 25.43 and 2.31% of all stations showed significant decreasing and increasing trends at 95% confidence level in summer. The number of stations with decreasing trends in spring, distributed in the northwest and northeast, was similar to the number displaying such trends in autumn, although these were located in the central and northwestern parts of the study area. In winter, the percentage of stations with significant increasing trends was the largest compared with other seasons, reaching 7.51%. These stations were mainly located in the central part of the study area.

3.3.2. Spatial distributions of meteorological variables trends

The spatial distributions of trends in annual meteorological variables from 1960 to 2013 indicated that MAT and MIT both had increasing trends at almost all stations (Figure 5). The magnitude of increasing annual MAT varied from 0.03 °C decade^{-1} at Keping to 0.42 °C decade^{-1} at Balikun, with an average increase of 0.16 °C decade^{-1}. The trends of MAT at 116 stations, located in the central, northwestern and southwestern parts of the study area, showed significant increasing trends, and 57 stations, concentrated in the northeast part of the study area, showed insignificant increasing trends. The magnitudes of increasing trends of annual MIT varied from 0.03 °C decade^{-1} at Alaer to 0.32 °C decade^{-1} at Habahe, with an average increase of 0.14 °C decade^{-1}. The trends of MIT at 123 stations, located more or less throughout the study area, showed significant increasing trends, while only 1 station, Kuche showed a significant decreasing trend. The annual RH, WS, and SH series were all characterized by mostly decreasing trends over much of the region. The average annual decrease in RH was −0.26% per decade. Annual RH at 129 stations, located in the central and northeast parts of the study area, showed decreasing

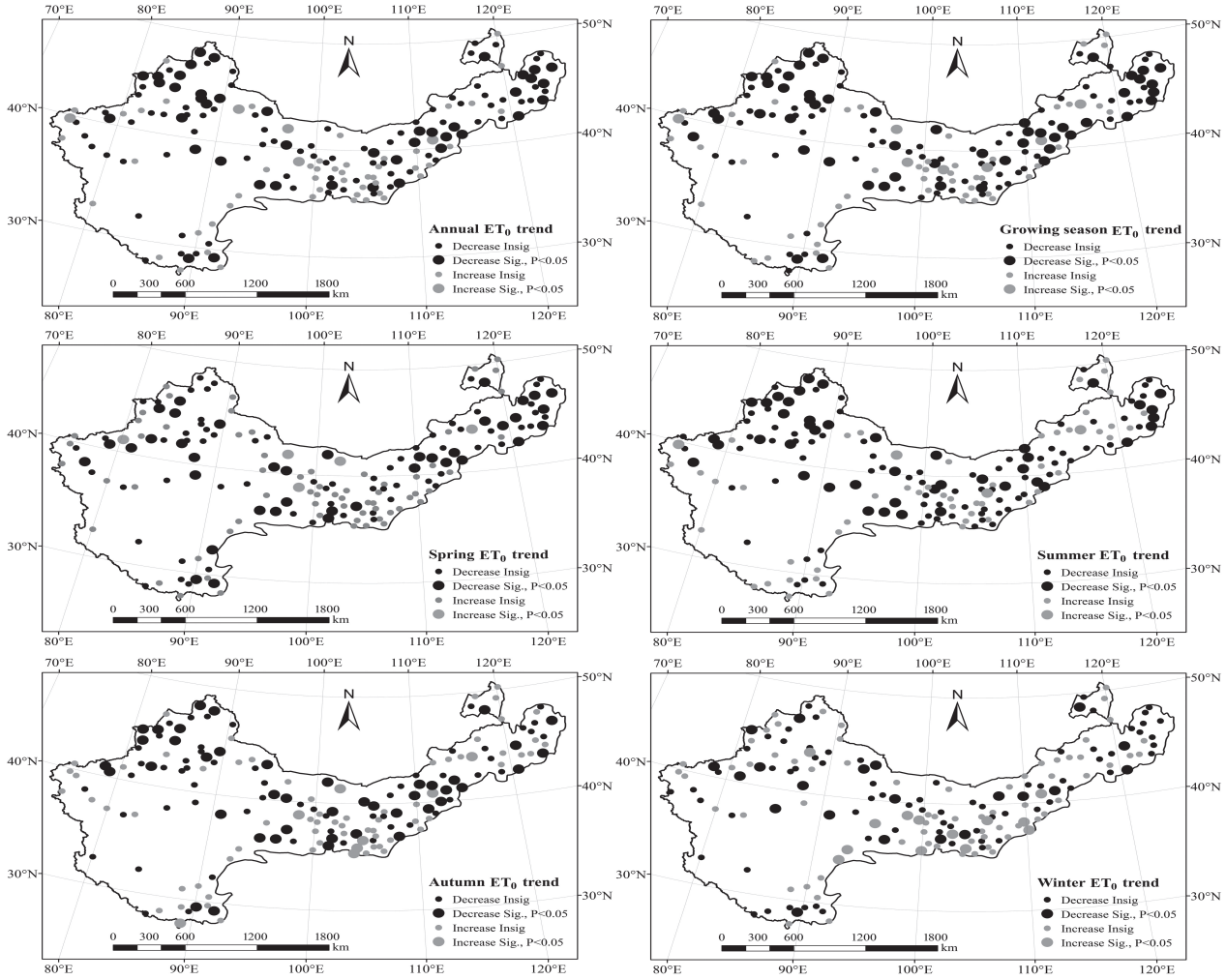

Figure 4. Spatial distributions of annual and seasonal ET_0 trends from 1960 to 2013.

trends, 49 stations of which were significant ($p < 0.05$) and accounted for 28.32% of all stations. Another 44 stations, found in the western part of the study area, showed increasing trends, 3 of which were significant ($p < 0.05$). Annual WS at 157 stations, located in the northwestern and northeastern parts of the study area, showed decreasing trends, 67 of which were significant and accounted for 38.73% of all stations. The average value of annual WS was $-0.14\,\mathrm{m\,s^{-1}}$ decade^{-1} and the greatest value was at Anduo, where the trend slope was $-0.57\,\mathrm{m\,s^{-1}}$ decade^{-1}. Annual SH at 131 stations, located in the eastern portion of the region, showed decreasing trends, 70 stations of which were significant decreasing trends accounting for 40.46% of all stations. Another 42 stations, located in the western part of the study area, had increasing trends, 2 of which were significant. The spatial distribution of annual P trend showed an increasing trend in most of the study area, with an average value of 2.07 mm decade^{-1}. Annual P at 115 stations, located in the western part of the study area, showed increasing trends. These trends were significant at 36 stations (20.81% of total). The increasing trend ranged from 0.03 mm decade^{-1} at Ejin Banner to 23.66 mm decade^{-1} at Urmuqi.

3.4. Influence of meteorological variables on ET_0 trend

3.4.1. Dominant factors affecting trends in ET_0

Dominant factors differed considerably in different timescales (Figure 6). WS was clearly the most dominant factor in the DPR throughout the study period. The annual ET_0 trend (-3.52 mm decade^{-1}) was dominated by wind speed ($-0.14\,\mathrm{m\,s^{-1}}$ decade^{-1}) at 132 stations, and the average contribution rate was 39.48%. MAT increased by 0.16 °C decade^{-1} and was the dominant factor at six stations, contributing 21.17%. During the growing season, the spatial distribution of dominant factors was similar to that of the annual scale. There were 132 stations where ET_0 was dominated by WS, and its average contribution rate was 37.33%. RH made the greatest contributions to the variation in ET_0 at 18 stations and SH at 17. In spring, ET_0 trends were dominated by WS at 99 stations and by MAT at 41 stations. The decrease in WS ($-0.18\,\mathrm{m\,s^{-1}}$ decade^{-1}) and the increase in temperature (0.19 °C decade^{-1}) caused a decrease in ET_0 (-1.08 mm decade^{-1}), with contributions of 33.13 and 27.17%, respectively. In summer, the number of stations dominated by SH increased, contributing 23.28%. These stations were mainly located in the eastern and central parts of the study area. WS dominated

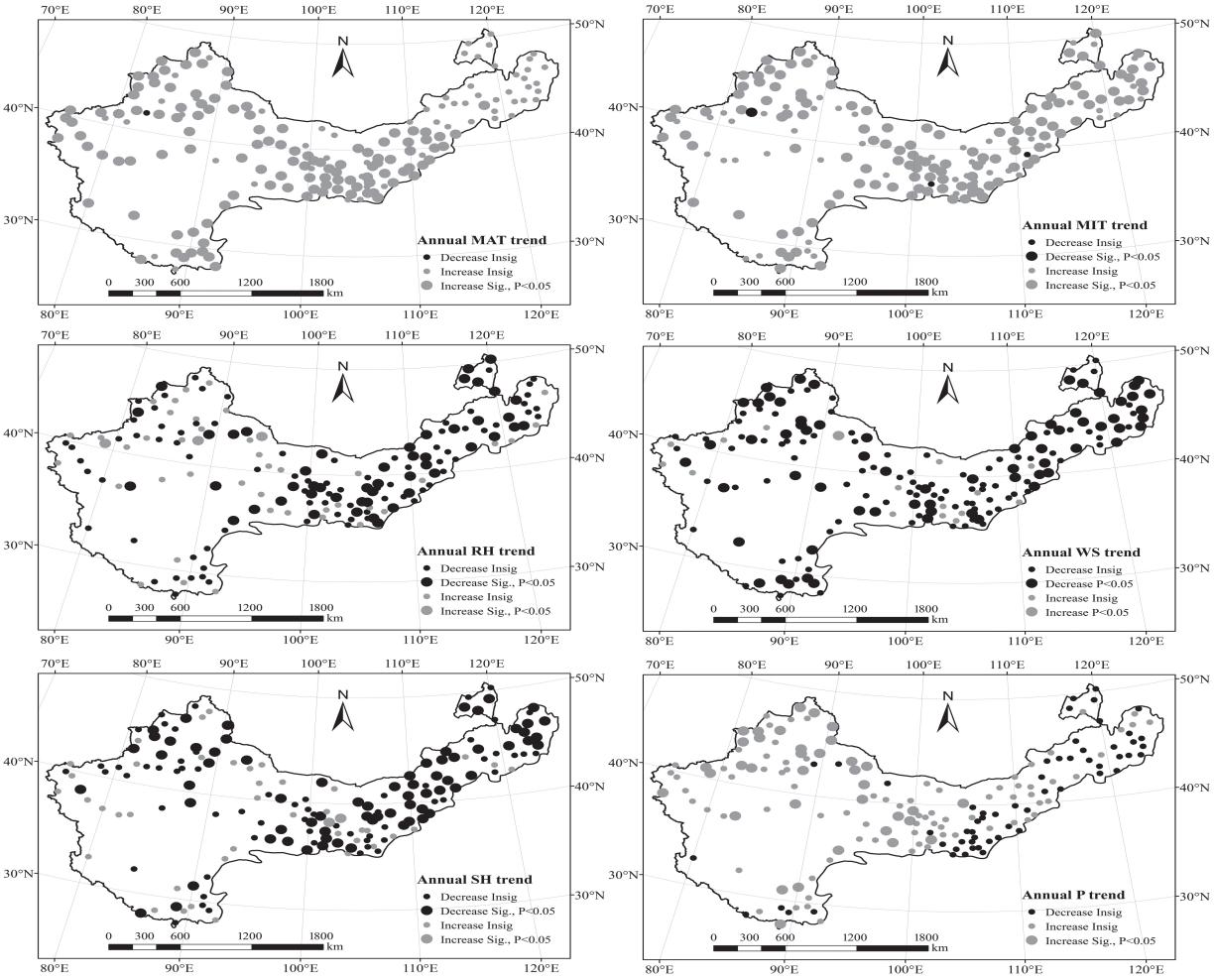

Figure 5. Spatial distributions of annual trends for MAT, MIT, RH, WS, SH, and P from 1960 to 2013.

ET_0 variation at 103 stations, contributing 34.16%. MAT (0.15 °C decade^{-1}) and RH (−0.24% per decade) also influenced ET_0. In autumn, WS was the most dominant factor at 131 stations and RH at 26. The contribution of WS was greatest in winter, when it accounted for 40.75%. RH was more likely to dominate changes in ET_0 in the eastern part of the study area, where it contributed 23.81%. In winter, the variation in ET_0 was dominated by WS and MAT, as in spring. WS contributed 35.34% and decreased by $-0.13\,\mathrm{m\,s^{-1}}$ decade^{-1}. MAT contributed 29.59% and stations where MAT dominated were mainly located in the eastern and northwestern parts of the study area.

3.4.2. Evaluation of the effect of wind speed on ET_0

Figure 6 illustrated that annual and seasonal ET_0 trends were dominated by decreasing wind speed at most stations. This may be due to the weak water vapour exchange caused by the lower WS. To further understand the influence of WS and other meteorological factors on changes in ET_0, the stations were grouped into seven categories based on the mean WS. Annual magnitudes of ET_0 and meteorological factors in different wind levels were illustrated in Table 1. Results demonstrated that the magnitudes of annual ET_0 trends generally increased as WS increased. Larger magnitudes occurred when WS was between 3.0 and 4.0 $\mathrm{m\,s^{-1}}$, which confirmed that stronger winds caused ET_0 to increase. In addition, more pronounced decreasing trend of SH also reduced the decrease of variations in ET_0 at wind speeds of 3.0–4.0 $\mathrm{m\,s^{-1}}$. However, when WS was above 4.0 $\mathrm{m\,s^{-1}}$ with the slope of $-0.07\,\mathrm{m\,s^{-1}}$ decade^{-1}, the magnitude of the ET_0 trend decreased considerably, which may be attributable to the decreasing SH, decreasing RH, and increasing P. All these could have slowed the decrease in ET_0.

3.5. Effect of altitude on ET_0 trend

Due to the wide geographic scope of this study, the stations were grouped into three categories based on the altitude: 50 stations were at low altitude (altitude ≤ 1000 m), 96 stations at medium altitude (1000 m < altitude ≤ 3000), and 27 stations at high altitude (altitude > 3000 m). Annual variations in ET_0 and meteorological factors at different altitudes from 1960 to 2013 were analysed. Annual ET_0 showed a decreasing trend at low and medium altitudes, with the largest and smallest magnitudes of trend, respectively (Table 2). However, it showed an increasing trend of 4.28 mm decade^{-1} at high altitudes. At low altitudes, the largest variations in WS and SH caused a more

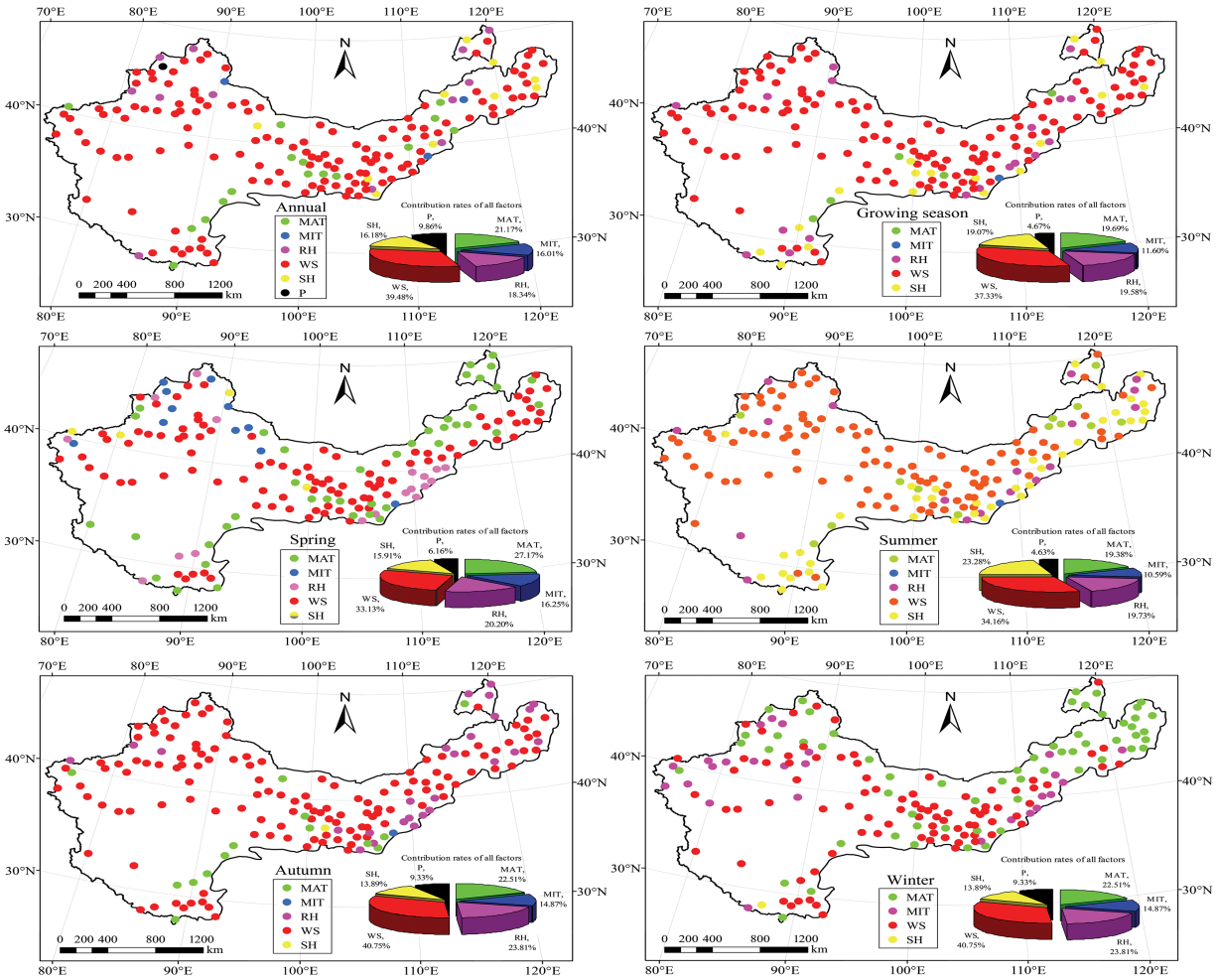

Figure 6. Spatial distributions of dominant factors of ET_0 change at different timescales.

Table 1. Magnitudes of trends in ET_0 and meteorological factors for different wind speeds ($m\,s^{-1}$) from 1960 to 2013.

Wind speed level	Number of stations	ET_0 ($mm\,decade^{-1}$)	WS ($m\,s^{-1}\,decade^{-1}$)	MAT ($°C\,decade^{-1}$)	MIT ($°C\,decade^{-1}$)	RH (% per decade)	SH ($h\,a^{-1}\,decade^{-1}$)	P ($mm\,decade^{-1}$)
WS < 1.5	9	−2.251	−0.11	0.191	0.102	−0.189	−2.259	0.968
1.5 ≤ WS < 2.0	28	−2.608	−0.11	0.189	0.107	−0.271	−13.501	3.274
2.0 ≤ WS < 2.5	40	−2.381	−0.10	0.172	0.139	−0.315	−13.726	4.171
2.5 ≤ WS < 3.0	31	−4.926	−0.16	0.155	0.143	−0.290	−12.869	1.306
3.0 ≤ WS < 3.5	28	−7.432	−0.19	0.106	0.156	−0.183	−22.430	0.310
3.5 ≤ WS < 4.0	22	−6.606	−0.25	0.147	0.180	−0.342	−18.960	0.964
WS ≥ 4.0	15	−2.995	−0.07	0.169	0.150	−0.077	−11.250	1.351

pronounced decrease in ET_0. At medium altitudes, the smaller variations in WS and SH trends caused ET_0 to decrease. At high altitudes, the ET_0 showed an increasing trend, which might due to the combined effect of lower WS, higher SH and P.

4. Discussion

In the DPR, trends in ET_0 were mixed. Spatially, most stations had decreasing trends, consistent with reports from other semi-arid and arid regions (Tabari *et al.*, 2012; Cruz-Blanco *et al.*, 2014; Jhajharia *et al.*, 2014). The average magnitude of decreasing trends in the DPR was $-3.52\,mm\,decade^{-1}$, larger than Heihe ($-0.71\,mm\,decade^{-1}$) (Xing *et al.*, 2014), and arid inland regions in northwestern China ($-3.41\,mm\,decade^{-1}$) (Huo *et al.*, 2013) but smaller than the Tibetan Plateau ($-17.4\,mm\,decade^{-1}$) (Zhang *et al.*, 2007), Qilian mountains and Hexi corridor ($-16.70\,mm\,decade^{-1}$) (Jia *et al.*, 2009), western Inner Mongolia ($12.20\,mm\,decade^{-1}$) (He *et al.*, 2013), southwestern China ($-5.00\,mm\,decade^{-1}$) (Li *et al.*, 2014a, 2014b), and Beijing-Tianjin sand source control project zone ($-3.80\,mm\,decade^{-1}$) (Shan *et al.*, 2015). ET_0 trends in this study were smaller than most

Table 2. Magnitudes of trends in ET_0 and meteorological factors at different altitudes in the DPR from 1960 to 2013.

Altitude (m)	ET_0 (mm decade^{-1})	MAT (°C decade^{-1})	MIT (°C decade^{-1})	RH (% per decade)	WS (m s^{-1} decade^{-1})	SH (ha^{-1} decade^{-1})	P (mm decade^{-1})
Low altitude	−7.287	0.149	0.149	−0.223	−0.17	−20.609	0.124
Medium altitude	−3.751	0.164	0.137	−0.324	−0.15	−14.525	1.677
High altitude	4.281	0.200	0.117	0.200	−0.10	4.029	9.677

reports in other parts of China (McVicar *et al.*, 2012). However, an increase in ET_0 was also detected in other semi-arid and arid regions. Dinpashoh *et al.* (2011) reported that most increasing trends in ET_0 were in the dry farming regions of northwest and northeast of Iran. There was still no conclusion on trends in ET_0 in different semi-arid and arid regions of the world.

ET_0 trends were dominated by different factors in different regions. Obviously, decreasing ET_0 at most stations was mainly due to the decrease in WS on annual and seasonal time scales, similar to other studies in the northwestern China (Huo *et al.*, 2013), Tibetan Plateau (Zhang *et al.*, 2007), and other semi-arid and arid regions (Chattopadhyay and Hulme, 1997; Dinpashoh *et al.*, 2011; Hoffman, *et al.*, 2011; Tabari *et al.*, 2012). In some humid regions, wind speed was the most influencing factor on evapouration (Jhajharia *et al.*, 2006, 2009).

Surface wind is an essential driving force behind continent–ocean dynamics and fluxes and it is strongly influenced by atmospheric circulations. Global warming can render differences in temperature between the poles and the equator, and thereby slow down global air circulation (Liuzzo *et al.*, 2014). A weakened Siberian High and East Asian Monsoon ultimately led to a decrease in wind speed (Yu *et al.*, 2004; Tubi and Dayan, 2013). Many studies have reported decreases in near-surface terrestrial wind speeds over the past several decades (McVicar *et al.*, 2008; Wan *et al.*, 2010; Hewston and Dorling, 2011). However, in specific areas, local wind speeds may increase due to increasing temperature (Hazlett, 2011; Rahim *et al.*, 2012).

Air temperature and solar radiation also contributed to changes in ET_0. Increasing trends in air temperature and decreasing trends in solar radiation may influence the upward and downward trends in ET_0, respectively. Global warming brought increases in temperature and increasing cloud cover led to global dimming (Stanhill and Cohen, 2001). Besides, the concentration of anthropogenic greenhouse gases, emission of aerosols and pollution, and urbanization, which all due to human activities, are also other primary factors affecting temperature warming and radiation dimming (Streets *et al.*, 2008; Ji and Zhou, 2011; Najafi *et al.*, 2015). A cooling effect attributable to irrigation has been detected in the arid/semi-arid region of China and contributes to decrease in ET_0 (Han *et al.*, 2014).

In this area, dust storms are a common phenomenon in spring. They are mainly controlled by soil moisture, wind speed, and vegetation conditions (Tan *et al.*, 2012). With the decreasing trend of ET_0 and increasing trend of P in the DPR, the increase in the amount of available water

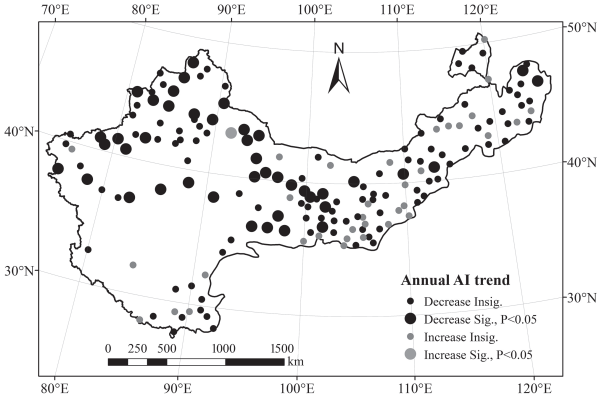

Figure 7. Trends of aridity index ($ET_0\,P^{-1}$) from 1960 to 2013.

may provide favourable conditions for plant growth and community establishment. Increasing trends in vegetation cover and soil moisture could help stabilize shifting dunes and reduce the number of surface particles in the air (Jiang *et al.*, 2006; Reynolds *et al.*, 2007). Under a lowered wind speed in this study, wind-blown sand was rare, and wind erosion did not happen. This reduced dust emissions and sandstorms frequency, which may have reduced the occurrence of sand desertification. The number of days with sandstorms had a decreasing trend from 1958 to 2007 in northern China. This suggests that the decreases in ET_0, WS, and increase in P contribute to a reduction of dust storms (Mao *et al.*, 2011).

Desertification is a process of land degradation induced by the excessive human activities and climate change in arid, semi-arid, and dry sub-humid areas (United Nations Convention to Combat Desertification (UNCCD), 2004), which results in an overall loss of ecosystem services and poses serious threats to sustainable living (D'Odorica *et al.*, 2013). To combat desertification, the government of China has launched a series of key ecological projects, such as the Three-North Shelterbelt Project, Beijing-Tianjin Sandstorm Source Control Project, and Returning Farmlands to Forest Project (Stokes *et al.*, 2010; Wang *et al.*, 2013). In the western part of the study area, decreasing ET_0 and increasing P trends usually led to increases in soil moisture and vegetation cover, preventing sand encroachment from an adjacent area and desertification expansion (Ffolliott *et al.*, 1995; Jiang *et al.*, 2006). In addition, a decrease in the aridity index (ratio between annual ET_0 and P) (Figure 7, Table 3) suggests that the climate is getting wetter (Huo *et al.*, 2013). This is especially evident in autumn and winter when the trends of aridity index decreased faster than that

Table 3. Trends in aridity index of different seasons in the DPR during 1960–2013.

Season	Spring	Summer	Autumn	Winter	Growing season	Annual
Aridity index	−0.36	−0.04	−058	−0.54	−0.05	−0.07

in the other seasons. The environmental conditions are favourable for implementation of ecological projects and restoration of regional vegetation, which may improve the condition of degraded land and reduce the degree of desertification (Wang, 2014). In summer, the greater decrease in ET_0 and lesser increase in P contributed to a decrease in the aridity index at the lowest magnitude. However, in the eastern part of the study area, an increasing trend was detected in the aridity index, resulting from decreasing trends in precipitation that were larger than that in ET_0. A drier climate tended to decrease the soil moisture and limit plant growth. This led to decreases in runoff and vegetation coverage, facilitating active desertification processes and accelerating environmental degradation (Martinez-Beltran and Manzur, 2005; Fisher *et al.*, 2011). All these limited the performance of ecological projects and vegetable restoration, and posed a disadvantage for ecological reconstruction and control of desertification.

Artificial irrigation is intensive in the DPR and expanding rapidly (Siebert *et al.*, 2005; Han *et al.*, 2014). Most important agricultural regions rely heavily on irrigation. ET_0 is the primary factor controlling irrigation water demand (Han *et al.*, 2014). Increasing P and decreasing ET_0 may increase soil moisture and decrease crop water demand, which suggests that less irrigation is needed to maintain crop growth (Ozdogan *et al.*, 2006). In return, a higher water requirement for crop may increase in ET_0 (Dinpashoh *et al.*, 2011). For this reason, it is necessary to understand the mechanism of relationship between ET_0 and irrigation in water-limited areas. The development of reasonable management strategies for water resource utilization requires considering hydrological components, such as ET_0, precipitation, and runoff. This might also help managers mitigate the desertification process, maintain ecological security and realize sustainable economic development in the context of climate change.

5. Conclusions

Temporal and spatial patterns in ET_0 and driving factors were evaluated for the period of 1960–2013 in the DPR. Results showed that the more ET_0 series had decreasing than increasing trends, particularly in the northeastern and northwestern parts of the region. The average ET_0 series in the DPR experienced a significant decrease before 1990s and increased slightly thereafter. Spatial variations of meteorological factors were evident in this study. Significant increasing trends were detected in MAT, MIT, and P. Significant decreasing trends were detected in relative humidity, wind speed, and hours of sunshine. Declines in ET_0 rates appeared to be related to decreasing annual, growing season, and autumnal wind speed. MAT contributed to the variation in ET_0 in spring and winter, and hours of sunshine also made a significant contribution to ET_0 in summer. The magnitude of the decreasing ET_0 trend increased till wind speed reached at a certain point, after it decreased. ET_0 had a decreasing trend at low altitudes but an increasing trend at high altitudes. Due to the increasing trend of precipitation, a wetter climate was observed in the western part of the study area. However, the decrease in precipitation led to a drier climate in the eastern part of the study area.

The results of this study may facilitate improved water and agricultural management plans, especially with respect to potential desertification. Better understanding of changes in ET_0 may be beneficial to agricultural productions and ecological restoration. However, more attention should be paid to evaluation of relationships between variations in ET_0 and meteorological variables. This could provide a scientific indicator for appropriate water management and adaptation strategies under the effects of global climate change.

Acknowledgements

This research was supported by grants from the '948' Project of State Forestry Administration P.R. China (2015-4-27), International S&T Cooperation Program of China (2015DFR31130), and National Natural Science Foundation of China (41271033, 41471029, and 41371500).

References

Allen RG, Periera LS, Raes D, Smith M. 1998. Crop evapotranspiration: guideline for computing crop water requirement. FAO irrigation and drainage. Paper No. 56, FAO, Rome, Italy.

Berti A, Tardivo G, Chiaudani A, Rech F, Borin M. 2014. Assessing reference evapotranspiration by the Hargreaves method in north-eastern Italy. *Agric. Water Manage.* **140**: 20–25.

Chattopadhyay N, Hulme M. 1997. Evaporation and potential evapotranspiration in India under conditions of recent and future climate change. *Agric. For. Meteorol.* **87**(1): 55–73.

Chinese Committee for Implementing UN Convention to Combat Desertification (CCICCD). 1997. *China Country Paper to Combat Desertification*. China Forestry Publishing House: Beijing.

Croitoru AZ, Piticar A, Dragotă CS, Burada DC. 2013. Recent changes in reference evapotranspiration in Romania. *Glob. Planet. Change* **11**: 127–132.

Cruz-Blanco M, Lorite IJ, Santos C. 2014. An innovative remote sensing based reference evapotranspiration method to support irrigation water management under semi-arid conditions. *Agric. Water Manage.* **131**: 135–145.

Dinpashoh Y, Jhajharia D, Fakheri-Fard A, Singh VP, Kahya E. 2011. Trends in reference crop evapotranspiration over Iran. *J. Hydrol.* **399**(3): 422–433.

D'Odorica P, Bhattachan A, Davis KF, Ravi S, Runyan CW. 2013. Global desertification: drivers and feedbacks. *Adv. Water Resour.* **51**(1): 326–344.

Espadafor M, Lorite IJ, Gavilán P, Berengeana J. 2011. An analysis of the tendency of reference evapotranspiration estimates and other climate variables during the last 45 years in Southern Spain. *Agric. Water Manage.* **98**: 1045–1061.

Feng J, Yan D, Li C, Yu F, Zhang C. 2014. Assessing the impact of climatic factors on potential evapotranspiration in droughts in North China. *Quart. Int.* **336**: 6–12.

Ffolliott PF, Gottfried GJ, Rietveld WJ. 1995. Dryland forestry for sustainable development. *J. Arid Environ.* **30**(2): 143–152.

Fisher JB, Whittaker RJ, Malhi Y. 2011. ET come home: potential evapotranspiration in geographical ecology. *Glob. Ecol. Biogeogr.* **20**: 1–18.

Gan T. 2000. Reducing vulnerability of water resources of Canadian Prairies to potential droughts and possible climate warming. *Water Resour. Manage.* **14**(2): 111–135.

Han S, Xu D, Wang S. 2012. Decreasing potential evaporation trends in China from 1956 to 2005: accelerated in regions with significant agricultural influence? *Agric. For. Meteorol.* **154–155**: 44–56.

Han S, Tang Q, Xu D, Wang S. 2014. Irrigation-induced changes in potential evaporation: more attention is needed. *Hydrol. Processes* **28**: 2717–2720.

Hazlett M. 2011. *Climate Change Could Have Major Impacts on Wind Resources*. North American Windpower, Zackin Publications Inc: Oxford, CT.

He D, Liu Y, Pan Z, An P, Wang L, Dong Z, Zhang J, Pan X, Zhao P. 2013. Climate change and its effect on reference crop evapotranspiration in central and western Inner Mongolia during 1961–2009. *Front. Earth Sci.* **7**(4): 417–428.

Hewston R, Dorling SR. 2011. An analysis of observed daily maximum wind gusts in the UK. *J. Wind Eng. Ind. Aerodyn.* **99**: 845–856.

Hoffman MT, Cramer MD, Gillson L, Wallace M. 2011. Pan evaporation and wind run decline in the Cape Floristic Region of South Africa (1974–2005): implications for vegetation responses to climate change. *Clim. Change* **109**: 437–452.

Huo Z, Dai X, Feng S, Kang S, Huang G. 2013. Effect of climate change on reference evapotranspiration and aridity index in arid region of China. *J. Hydrol.* **492**: 24–34.

Irmak S, Kabenge I, Skaggs KE, Mutiibwa D. 2012. Trend and magnitude of changes in climate variables and reference evapotranspiration over 116-yr period in the Platte River Basin, central Nebraska–USA. *J. Hydrol.* **420–421**: 228–244.

Jhajharia D, Kithan SB, Fancon AK. 2006. Correlation between pan evaporation and meteorological parameters under the climatic conditions of Jorhat (Assam). *J. Indian Water Resour. Soc.* **26**(1 & 2): 39–42.

Jhajharia D, Agrawal G, Sevda MS. 2009. Influence of meteorological parameters on pan evaporation at Agartala. *J. Agric. Eng.* **46**(1): 23–26.

Jhajharia D, Dinpashoh Y, Kahya E, Singh VP, Fakher-Fard A. 2012. Trends in reference evapotranspiration in the humid region of northeast India. *Hydrol. Processes* **26**: 421–435.

Jhajharia D, Kumar R, Dabral PP, Singh VP, Choudhary RR, Dinpashoh Y. 2014. Reference evapotranspiration under changing climate over the Thar Desert in India. *Meteorol. Appl.* **22**(3): 425–435, doi: 10.1002/met.1471.

Ji Y, Zhou G. 2011. Important factors governing the incompatible trends of annual pan evaporation: evidence from a small scale region. *Clim. Change* **106**: 303–314.

Jia W, He Y, Wang X, Li Z. 2009. Temporal and spatial change of the potential evaporation over Qilian mountains and Hexi corridor from 1960 to 2006. *Adv. Water Sci.* **20**(2): 159–167 (in Chinese).

Jiang G, Han X, Wu J. 2006. Restoration and management of the Inner Mongolia grassland require a sustainable strategy. *Ambio* **35**(5): 269–270.

Jung M, Reichstein M, Ciais P, Seneviratne SI, Sheffield J. 2010. Recent decline in the global land evapotranspiration trend due to limited moisture supply. *Nature* **467**: 951–954.

Kendall MG. 1975. *Rank Correlation Methods*. Griffin: London.

Kosmas C, Tsara M, Moustakas N, Karavitis C. 2003. Identification of indicators for desertification. *Ann. Arid Zone* **42**: 393–416.

Kousari MR, Ahani H. 2012. An investigation on reference crop evapotranspiration trend from 1975 to 2005 in Iran. *Int. J. Climatol.* **32**(15): 2387–2402.

Li Z, Chen Y, Yang J, Wang Y. 2014a. Potential evapotranspiration and its attribution over the past 50 years in the arid region of Northwest China. *Hydrol. Processes* **28**: 1025–1031.

Li Z, Feng Q, Liu W, Wang T, Gao Y, Wang Y, Cheng A, Li J, Liu L. 2014b. Spatial and temporal trend of potential evapotranspiration and related driving forces in Southwestern China, during 1961–2009. *Quart. Int.* **336**: 127–144.

Li S, Yu F, Werger Marinus JA, Dong M, During HJ, Zuidema P. 2015. Mobile dune fixation by a fast-growing clonal plant: a full life-cycle analysis. *Sci. Rep.* **5**: 8935.

Limjirakan S, Limsakul A. 2012. Trends in Thailand pan evaporation from 1970 to 2007. *Atmos. Res.* **108**: 122–127.

Liuzzo L, Viola F, Noto LV. 2014. Wind speed and temperature trends impacts on reference evapotranspiration in Southern Italy. *Theor. Appl. Climatol.* 1–20, doi: 10.1007/s00704-014-1342-5.

Ma Z, Li D, Hu Y. 2004. The extreme dry/wet events in northern China during recent 100 years. *J. Geogr. Sci.* **14**(3): 275–281.

Mann HB. 1945. Non-parametric tests against trend. *Econometrica* **33**: 245–259.

Mao R, Gong D, Bao J, Fan Y. 2011. Possible influence of Arctic Oscillationon dust storm frequency in North China. *J. Geogr. Sci.* **21**(2): 207–218.

Martinez-Beltran J, Manzur CL. 2005. Overview of salinity problems in the world and FAO strategies to address the problem. In *Proceedings of the International Salinity Forum*, Riverside, CA, 25–27 April 2005, 311–314.

McVicar TR, Niel TGV, Li L, Michael LR, Rayner DP. 2008. Wind speed climatology and trends for Australia, 1975–2006: capturing the stilling phenomenon and comparison with near-surface reanalysis output. *Geophys. Res. Lett.* **35**(20): 288–299.

McVicar TR, Roderick ML, Donohue RJ, Li LT, Van Niel TG, Thomas A, Grieser J, Jhajharia D, Himri Y, Mahowald NM, Mescherskaya AV, Kruger AC, Rehman S, Dinpahoh Y. 2012. Global review and synthesis of trends in observed terrestrial near-surface wind speeds: implications for evaporation. *J. Hydrol.* **416–417**: 182–205.

Middleton NJ, Thomas D. 1997. *World Atlas of Desertification*. Arnold Publication, United Nations Environment Programme: London.

Najafi MR, Zwiers FW, Gillett NP. 2015. Attribution of Arctic temperature change to greenhouse-gas and aerosol influences. *Nat. Clim. Change* **5**: 246–249.

Nam WH, Hong EM, Choi JY. 2015. Has climate change already affected the spatial distribution and temporal trends of reference evapotranspiration in South Korea? *Agric. Water Manage.* **150**: 129–138.

Ozdogan M, Woodcock CE, Salvucci GD, Demir H. 2006. Changes in summer irrigated crop area and water use in Southeastern Turkey from 1993 to 2002: implications for current and future water resources. *Water Resour. Manage.* **20**: 467–488.

Rahim M, Yoshino J, Doi Y, Yasuda T. 2012. Effects of global warming on the average wind speed field in Central Japan. *J. Sustain. Energy Environ.* **3**: 165–171.

Rayner DP. 2007. Wind run changes: the dominant factor affecting pan evaporation trends in Australia. *J. Clim.* **20**: 3379–3394.

Reynolds JF, Smith DM, Lambin EF, Turner BL 2nd, Mortimore M, Batterbury SP, Downing TE, Dowlatabadi H, Fernandez RJ, Herrick JE, Huber-Sannwald E, Jiang H, Leemans R, Lynam T, Maestre FT, Ayarza M, Walker B. 2007. Global desertification: building a science for dryland development. *Science* **316**(5826): 847–851.

Roderick ML, Farquhar GD. 2005. Changes in New Zealand pan evaporation since 1970s. *Int. J. Climatol.* **25**: 2031–2039.

Salmi T, Maatta A, Anttila P, Ruoho-Airola T, Amnell T. 2002. *Detecting Trends of Annual Values of Atmospheric Pollutants by the Mann-Kendall Test and Sen's Slope Estimates – the Excel Template Application MAKESENS* no 31, FMI-AQ-31. Finnish Meteorological Institute: Helsinki.

Sen PK. 1968. Estimates of the regression coefficient based on Kendall's tau. *J. Am. Stat. Assoc.* **63**: 1379–1389.

Shadmani M, Marofi S, Roknian M. 2012. Trend analysis in reference evapotranspiration using Mann-Kendall and Spearman's Rho tests in arid regions of Iran. *Water Resour. Manage.* **206**: 211–224.

Shan N, Shi Z, Yang X, Gao J, Cai D. 2015. Spatiotemporal trends of reference evapotranspiration and its driving factors in the Beijing–Tianjin sand source control project region, China. *Agric. For. Meteorol.* **200**(15): 322–333.

Sharifi A, Dinpashoh Y. 2014. Sensitivity analysis of the Penman-Monteith reference crop evapotranspiration to climatic variables in Iran. *Water Resour. Manage.* **28**: 5465–5476.

Siebert S, Döll P, Hoogeveen J, Faures JM, Frenken K, Feick S. 2005. Development and validation of the global map of irrigation areas. *Hydrol. Earth Syst. Sci.* **9**: 535–547.

Stanhill G, Cohen S. 2001. Global dimming: a review of the evidence for a widespread and significant reduction in global radiation with discussion of its probable causes and possible agricultural consequences. *Agric. For. Meteorol.* **107**: 255–278.

Stokes A, Sotir R, Chen W, Chestem M. 2010. Soil bio- and eco-engineering in China: past experience and future priorities preface. *Ecol. Eng.* **36**: 247–257.

Streets D, Yu C, Wu Y, Chin M, Zhao Z, Hayasaka T, Shi G. 2008. Aerosol trends over China, 1980–2000. *Atmos. Res.* **88**: 174–182.

Tabari H, Aeini A, Hosseinzadeh Talaee P, Shifteh Some'e B. 2012. Spatial distribution and temporal variation of reference evapotranspiration in arid and semi-arid regions of Iran. *Hydrol. Processes* **26**: 500–512.

Tan S, Shi G, Wang H. 2012. Long-range transport of spring dust storms in Inner Mongolia and impact on the China seas. *Atmos. Environ.* **46**: 299–308.

Theil H. 1950. A rank-invariant method of linear and polynomial regression analysis. Part 3. In *Proceedings of Koninalijke Nederlandse Akademie van Weinenschatpen A*, **53**: 1397–1412.

Tubi A, Dayan U. 2013. The Siberian High: teleconnections, extremes and association with the Icelandic Low. *Int. J. Climatol.* **33**(6): 1357–1366.

UNCCD. 2004. *Preserving Our Common Ground. UNCCD 10 Years on*. United Nations Convention to Combat Desertification: Bonn, Germany.

Von Storch H. 1995. Misuses of statistical analysis in climate research. In *Analysis of Climate Variability: Applications of Statistical Techniques*, Storch HV, Navarra A (eds). Springer: Berlin, 11–26.

Wan H, Wang X, Swail VR. 2010. Homogenization and trend analysis of Canadian near-surface wind speeds. *J. Clim.* **23**: 1209–1225.

Wang T. 2014. Aeolian desertification and its control in Northern China. *Int. Soil Water Conserv. Res.* **2**(4): 34–41.

Wang S, Wang J, Zhou Z, Shang K. 2005. Regional characteristics of three kinds of dust storm events in China. *Atmos. Environ.* **39**(3): 509–520.

Wang P, Yamanaka T, Qiu G. 2012. Causes of decreased reference evapotranspiration and pan evaporation in the Jinghe River catchment, northern China. *Environmentalist* **32**: 1–10.

Wang F, Pan X, Wang D, Shen C, Lu Q. 2013. Combating desertification in China: past, present and future. *Land Use Policy* **31**: 311–313.

Wang Z, Wu P, Zhao X, Cao X, Gao Y. 2014. GANN models for reference evapotranspiration estimation developed with weather data from different climatic regions. *Theor. Appl. Climatol.* **116**(3–4): 481–489.

Wu B, Su Z, Chen Z. 2007. A revised potential extent of desertification in China. *J. Desert Res.* **27**(6): 911–917.

Xing W, Wang W, Shao Q, Peng S, Yu Z, Yong B, Taylor J. 2014. Changes of reference evapotranspiration in the Haihe River Basin: present observations and future projection from climatic variables through multi-model ensemble. *Glob. Planet. Change* **115**: 1–15.

Xu C, Gong LB, Jiang T, Chen D, Singh VP. 2006. Analysis of spatial distribution and temporal trend of reference evapotranspiration and pan evaporation in Changjiang (Yangtze River) catchment. *J. Hydrol.* **327**: 81–93.

Yin Y, Wu S, Dai E. 2010. Determining factors in potential evapotranspiration changes over China in the period 1971–2008. *Chin. Sci. Bull.* **55**(29): 3329–3337.

Yu R, Wang B, Zhou T. 2004. Tropospheric cooling and summer monsoon weakening trend over East Asia. *Geophys. Res. Lett.* **31**(22): 217–244.

Yue S, Wang C. 2004. The Mann-Kendall test modified by effective sample size to size to detect trend in serially correlated hydrological series. *Water Resour. Manage.* **18**: 201–218.

Zhang Y, Liu C, Tang Y, Yang Y. 2007. Trends in pan evaporation and reference and actual evapotranspiration across the Tibetan Plateau. *J. Geophys. Res.* **112**(D12): 1103–1118.

